http://dx.doi.org/10.5935/0103-5053.20140009

J. Braz. Chem. Soc., Vol. 25, No. 4, 619-628, 2014.
Printed in Brazil - ©2014 Sociedade Brasileira de Química
0103 - 5053 $6.00+0.00

Article

A Novel Computational Approach for Development of Highly Selective Fenitrothion Imprinted Polymer: Theoretical Predictions and Experimental Validations

Leonardo Augusto de Barros,[a] Leandro Alves Pereira,[a] Rogério Custódio[b] and Susanne Rath[*,a]*

[a]*Department of Analytical Chemistry and* [b]*Department of Physical Chemistry, Institute of Chemistry, University of Campinas, P.O. Box 6154, 13084-971 Campinas-SP, Brazil*

A qualidade dos sítios de reconhecimento molecularmente impressos dependem dos mecanismos e da extensão das interações monômero funcional-molde presentes na mistura de pré-polimerização. Assim, a compreensão dos parâmetros físicos que governam estas interações é a chave para a produção de um polímero de impressão molecular (MIP) altamente seletivo. Neste trabalho, novos estudos de modelagem molecular foram realizados para otimizar as condições de impressão molecular de fenitrotiona. Foram avaliados quatro possíveis monômeros funcionais. Cinco solventes porogênicos foram investigados utilizando o método da polarização contínua. O MIP baseado em ácido metacrílico (MAA-MIP) sintetizado na presença de tolueno demonstrou ser o complexo mais termodinamicamente estável. Ao contrário, MIP com base em ácido *p*-vinilbenzóico (PVB-MIP) teve a menor energia de ligação. De acordo com os parâmetros de adsorção ajustados pela isoterma de Langmuir-Freundlich, MIP-MAA apresentou duas vezes o número de sítios de ligação em comparação com o PVB-MIP (103,35 e 53,77 μmol g^{-1}, respectivamente).

The quality of molecularly imprinted recognition sites depend on the mechanisms and the extent of the functional monomer-template interactions present in the prepolymerization mixture. Thus, an understanding of the physical parameters governing these interactions is key for producing a highly selective molecularly imprinted polymer (MIP). In this paper, novel molecular modeling studies were performed to optimize the conditions for the molecular imprinting of fenitrothion. Four possible functional monomers were evaluated. Five porogenic solvents were investigated employing the polarizable continuum method. The MIP based in methacrylic acid (MAA-MIP) synthesized in the presence of toluene shown to be the most thermodynamically stable complex. Contrarily, MIP based in *p*-vinylbenzoic acid (PVB-MIP) had the lowest binding energy. According to the adsorption parameters fitted by the Langmuir-Freundlich isotherm, MAA-MIP presented twice the number of binding sites compared to PVB-MIP (103.35 and 53.77 μmol g^{-1}, respectively).

Keywords: molecularly imprinted polymer, molecular modeling, Gibbs free energy, functional monomer, solvent effect

Introduction

Molecularly imprinted polymers (MIPs) are considered important synthetic receptors due to their high affinity for a template molecule that is employed during the synthesis of these materials.[1,2]

Prior to MIP synthesis, it is important to select an appropriate functional monomer (FM), i.e., with complementar functionality in relation to the template to favor the formation of the complex FM-template.[3] The formation of covalent bonds between the FM and template molecule allows the establishment of more defined and homogeneous binding sites.[4]

Nevertheless, MIPs based on noncovalent interactions (e.g., electrostatic, hydrogen bonding, π-π and hydrophobic interactions) are more common than those based on covalent bonds because of the relatively simple experimental approach and the vast number of compounds capable of forming noncovalent interactions with polymerizable monomers.[4,5]

Recently, molecular modeling studies have been employed to MIP synthesis to identify a FM that interacts strongly with the template molecule and to select a porogenic solvent that enables the formation of a MIP with high selectivity and capacity. Computational approaches

*e-mail: raths@iqm.unicamp.br

using density functional theory (DFT) have been routinely used to calculate binding energies.[1,2,6-16] Due to its greater computational speed and acceptable chemical accuracy, this method is more attractive when compared with Hartree-Fock calculations.[13,17]

The computational approach is comprised of the separate optimization of conformations of the template (and/or its analogues) and FM, followed by the calculation of the energy (E) of each molecule. The same process is repeated for the FM-template complex. Finally, the binding energy (ΔE) is obtained from equation 1:

$$\Delta E = E_{complex} - E_{template} - nE_{monomer} \quad (1)$$

This methodology was employed in studies conducted by Farrington and Regan,[11] Liu *et al.*,[2] Yao *et al.*,[9] Wu *et al.*,[13] Dong *et al.*[7] and Chen *et al.*.[18] However, the use of Gibbs free energy (ΔG) to estimate the binding energies between two entities was taken into consideration in the 1990s because this parameter is more comprehensive and involves the values of enthalpy, entropy and temperature.[19-22] Furthermore, ΔG is the determinant thermodynamic criterion for a spontaneous process.

In general, molecular modeling studies have been focused on evaluating the interaction between the template and the FM. Only a few papers reported in the literature included the solvent effect in their calculations. It is worth emphasizing that during the polymerization, the extent of the noncovalent pre-polymer complex is affected by the polarity of the solvent[3,9,23] and that the porogen solvent should not dissociate the interactions formed between the FM and the template.[2] Modeling the solvation effect has been performed using the polarizable continuum model (PCM).[8,13,24,25]

The aim of the present study was to develop a MIP for the determination of fenitrothion (FNT), an organophosphate insecticide widely employed in agriculture, by selecting the optimal conditions using molecular modeling. For this purpose, the density functional theory, at the B3LYP/6-31G(d) level, and the PCM were adopted. To validate the theoretical results, FNT-imprinting was synthesized with two functional monomers (methacrylic acid and *p*-vinyl benzoic acid) and in three solvents (toluene, dichloromethane and acetonitrile) and subjected to the adsorption of FNT. Finally, the polymers synthesized were characterized using Fourier transform infrared spectroscopy (FT-IR), scanning electron microscopy (SEM), cross polarization magic angle spinning nuclear magnetic resonance (^{13}C CP-MAS NMR) and nitrogen sorption porosimetry (Brunauer-Emmet-Teller (BET) and Barrett-Joyner-Halenda (BJH)). Batch rebinding studies were performed to check the MIP selectivity in comparison with a non-imprinted polymer (NIP) and to evaluate the theoretical results obtained. Additionally, isotherms were adjusted to the Langmuir-Freundlich model.

Experimental

Materials and reagents

Fenitrothion (99%) was obtained from Chem Service (West Chester, PA, USA). Methacrylic acid (MAA), *p*-vinyl benzoic acid (PVB) and ethyleneglycol dimethacrylate (EGDMA) were obtained from Fluka (Buchs, Switzerland). The radical initiator 2,2'-azobis-iso-butyronitrile (AIBN) was obtained from Sigma-Aldrich (Munich, Germany). All of the reagents were used without further purification and were at least of analytical grade. HPLC grade solvents acetonitrile (ACN) and dichloromethane (DCM) were obtained from Tedia (Fairfield, OH, USA), and methanol (MeOH) was obtained from JT Baker (Phillipsburg, NJ, USA). Toluene was obtained from Synth (São Paulo, SP, Brazil), and acetic acid was obtained from Nuclear (São Paulo, SP, Brazil). Throughout the study, water was obtained from a Milli-Q system from Millipore (São Paulo, SP, Brazil). Before HPLC analyses, samples were filtered through a 0.22 μm nylon filter from Millipore.

Molecular modeling studies

Molecular modeling simulation was performed using Gaussian 03 software.[26] All the structures were minimized to the lowest energy conformation in vacuum at the B3LYP/6-31G(d) level. Subsequently, the harmonic vibrational frequencies were calculated. Thus, the electronic, vibrational, rotational and translational entropies and enthalpies of each molecule were obtained at 298.15 K. The same process was repeated with the FM-FNT complexes. Finally, the FM-FNT binding energy of each complex was estimated from ΔG.

Initially, FNT, FM, and FM-FNT absolute internal energies (U_T) were obtained from Gaussian 03 according to equation 2:

$$U_T(\text{kcal mol}^{-1}) = U_0 + U_{vib} + U_{rot} + U_{transl} + U_{electronic} \quad (2)$$

where U_0 is the zero-point energy; $U_{electronic}$ is the optimized energy; and U_{vib}, U_{rot} and U_{transl} are the vibrational, rotational and translational thermal energies, respectively.

For the calculation of the internal energy (ΔU), the FNT absolute internal energy $U_{T_{FNT}}$ and the FM absolute internal energy $U_{T_{FM}}$ were subtracted from the complex absolute internal energy $U_{T_{FM-FNT}}$.

$$\Delta U(\text{kcal mol}^{-1}) = U_{T_{FM-FNT}} - U_{T_{FNT}} - U_{T_{FM}} \quad (3)$$

Then, ΔH was obtained from equation 4:

$$\Delta H(\text{kcal mol}^{-1}) = \Delta U + (\Delta n \times R \times T) \quad (4)$$

where Δn is the change in the amount of substance in the reaction, *R* is the universal gas constant and *T* is the temperature.

The total entropy (S_T) of FNT, FM and FM-FNT was determined as follows:

$$S_T(\text{cal mol}^{-1}\ \text{K}^{-1}) = S_{vib} + S_{rot} + S_{transl} \quad (5)$$

where S_{vib}, S_{rot} and S_{transl} are the vibrational, rotational and translational entropies, respectively.

The variation of entropy (ΔS) was found by subtracting the FNT total entropy and FM total entropy from the complex total entropy :

$$\Delta S(\text{cal mol}^{-1}\ \text{K}^{-1}) = S_{FM-FNT} - S_{FNT} - S_{FM} \quad (6)$$

Finally, ΔG was obtained from:

$$\Delta G(\text{kcal mol}^{-1}) = \Delta H - \left(\frac{T \times \Delta S}{1000}\right) \quad (7)$$

Additionally, the solvent effect (γ) for five different solvents (toluene, dichloromethane, acetonitrile, tetrahydrofuran and water) was evaluated using the polarizable continuum model (PCM).[9,13] The solvent energy was estimated through ΔG, which was estimated using equation 8:

$$\gamma = \Delta G_{solution} - \Delta G_{vacuum} \quad (8)$$

A higher γ indicates a stronger affinity of the FM-FNT complex to the solvent and thus infers a higher degree of formation of the complex.

Square-wave voltammetry measurements

The FNT contents in the solutions used for the batch rebinding studies were determined by square-wave voltammetry (SWV) using an Autolab PGSTAT 30 potentiostat/galvanostat (Eco Chemie, Utrecht, The Netherlands) interfaced with a computer and controlled by GPES 4.0 software. A hanging mercury drop electrode (HMDE, area 0.52 mm^2) was used as the working electrode. Platinum wire and Ag/AgCl, KCl 3 mol L^{-1} were used as counter and reference electrodes, respectively.

pH measurements were obtained with a DM-20 pH meter from Digimed (São Paulo, Brazil) using a combined glass electrode.

The square wave voltammetric conditions used for the determination of FNT were described in a previous work and are as follows: frequency: 250 s^{-1}; pulse amplitude: 40 mV and scan rate: 200 mV s^{-1}. FNT quantitation was performed through external standardization using calibration graphs. The peak current intensities for FNT were measured at –0.35 V vs. Ag/AgCl, KCl 3 mol L^{-1}. The linear range of the calibration graph was from 0.5×10^{-5} to 3.0×10^{-5} mol L^{-1} with a linearity higher than 0.999.[27]

Polymer synthesis

MIPs were prepared by bulk polymerization, according to the non-covalent approach. FNT (0.5 mmol) as template, MAA or PVB (2 mmol) as functional monomer, EGDMA (8 mmol) as a cross-linker and AIBN (1.2 mmol) as a free radical initiator were dissolved in 3 mL solvent (toluene, DCM or ACN) in a 75 mL thick-walled glass tube. The mixture was homogenized in an ultrasonic bath and purged with oxygen-free nitrogen for 10 min. The glass tube was sealed with Parafilm under nitrogen, and polymerization was carried out in a thermostated oil bath at 65 °C for 24 h. The monolithic polymer obtained was crushed, ground and sieved (using a 250 mesh sieve). To remove the template from the polymer, the material was washed several times with MeOH:acetic acid (90:10, v/v) until FNT could no longer be detected in the solution by the previously established voltammetric method. Finally, acetic acid was removed from the polymer by percolating in 250 mL methanol. The polymer was dried overnight at 60 °C and stored at room temperature in a desiccator over silica gel. Non-imprinted polymers were prepared under identical conditions, except that there was no template present during the polymerization process.

Polymer characterization

Fourier transform infrared (FT-IR) spectroscopy

Polymer FT-IR spectra were obtained in 1% KBr pellets in an ABB Bomem (Quebec, Canada) MB Series spectrometer (model B100) between 4000-400 cm^{-1} with a resolution of 4 cm^{-1}.

Cross polarization magic angle spinning nuclear magnetic resonance (CP-MAS NMR)

NMR spectra (^{13}C CP-MAS) were recorded on a Bruker Avance II 400 MHz from Bruker Bio Spin (Rheinstetten, Germany) at 300 MHz with a contact time of 4 ms,

repetition interval of 3 s and acquisition signal time of 50 ms.

Scanning electron microscopy (SEM)

Particle size analyses were performed using a JEOL 6360 LV-JSM (Tokyo, Japan) instrument operating at 15 keV. Polymer particles were sputter-coated with gold up to a thickness of 12 nm in a Bal-Tec MED 020 (Balzers, Liechtenstein) coater prior to obtaining the SEM measurements.

Brunauer-Emmett-Teller (BET) analysis

The pore size distribution and surface areas of the washed polymers were measured by a multipoint Brunauer-Emmett-Teller (BET) analysis carried out on Quantachrome Analysis® equipment at cryogenic temperatures. Pore volume and average pore diameter were determined by the multipoint BJH (Barret-Joyner-Halenda) model on desorption. Adsorption and desorption isotherms were built to provide relevant information about the surface area, total pore volume and average pore diameter of the polymers.

Batch rebinding studies

Batch rebinding studies were performed for two purposes: to evaluate the molecular modeling predictions related to the interaction energy between FM-FNT using a solvent mixture of toluene:ACN (80:20, v/v) and to validate the molecular modeling predictions related to the solvent effect using a solvent mixture of toluene:ACN (80:20, v/v), DCM:ACN (80:20, v/v) or DCM:ACN (70:30, v/v). For the first purpose, fifty milligram quantities of dry polymer (MIP or NIP synthesized with MAA or VPB, in toluene) were transferred to 15 mL glass flasks, and 3 mL of a solution of FNT 3 mmol L^{-1}, prepared in toluene:ACN (80:20, v/v), were added. For the second purpose, fifty milligram quantities of dry polymer (MIP or NIP synthesized in toluene, DCM or ACN with MAA as functional monomer) were transferred to 15 mL glass flasks, and 3 mL of a solution of 3 mmol L^{-1}, prepared in each solvent mixture, were added. Then, the flasks were properly sealed, and the mixture was incubated under agitation in a horizontal shaker from Fanem (São Paulo, Brazil), model 315E, for 24 h. Aliquots of the supernatant were collected, and the FNT was quantified by SWV as described in the SWV measurements section. The data were analyzed using the computational software Origin 8 from OriginLab Corporation (Northampton, MA, USA).

Adsorption isotherms

Batch rebinding studies were performed to construct the adsorption isotherms for the polymers synthesized using the functional monomers MAA and PVB in toluene. Fifty milligram quantities of dry polymer (MIP or NIP) were transferred to 15 mL glass flasks, and 3 mL of a solution of FNT (concentration varying from 0.5 to 7.5 mmol L^{-1}), prepared in each solvent mixture, were added. The same procedure described previously in the previous section was followed. The adsorption isotherms were fitted using the computational software Origin 8 from OriginLab Corporation (Northampton, MA, USA).

Selectivity of MIP by solid phase extraction

Besides FNT, three structurally related compounds, parathion (PT), methylparathion (MPT) and fenthion (FT), were employed to evaluate the selectivity of the imprinted polymer at the determination of FNT in tomatoes using a solid phase extraction procedure as described in a previous work.[28] For this purpose blank tomato samples (5.0 g) were fortified with FNT, PT, MPT and FT at a concentration level of 1.000 μg g^{-1}.

Results and Discusssion

Theoretical selection of the functional monomer

The molecular structure of FNT shows two possible binding sites for the complexation with the FM: a nitro (NO_2) and a phosphorothionate (O_3PS) group. Thus, the formation of two complexes at these two binding sites was considered in the calculations. The proportion 1:1 FM:FNT was maintained.

The optimized geometries of functional monomer-template complexes (1:1) between MAA-FNT, AAD(acrylamide)-FNT, PVB-FNT and AAN(allylamine)-FNT are shown in Figure 1.

The calculated binding energies of FNT with the functional monomers MAA, AAD, PVB and AAN are

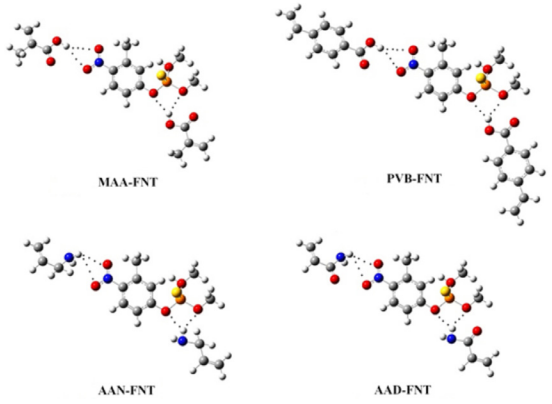

Figure 1. Optimized geometries of the most stable 1:1 complexes of FNT with MAA, PVB, AAN and AAD.

presented in Table 1. The results obtained show that MAA forms a more stable complex with FNT compared with AAN, AAD and PVB. Through the obtained structures and the calculated stabilization energies it is possible to consider that the effects of charge delocalization are important to justify the lower stability of the PVB-FNT complex in relation to MAA-FNT. For the other two complexes, hydrogen bond occurs between O···H–N, which are weaker than the O···H–O. In light of the obtained results, MAA was chosen as FM for the MIP synthesis.

Table 1. Gibbs energies of NO_2 and O_3PS groups (ΔG) and average Gibbs energies (ΔG_m) of the 1:1 complexes of fenitrothion with MAA, AAD, PVB and AAN.

Complexes	ΔG / (kJ mol^{-1})		ΔG_m / (kJ mol^{-1})
	NO_2 Group	O_3PS Group	
MAA-FNT	–2488.8	–2475.7	–2482.3
AAD-FNT	–2467.5	–2443.8	–2455.7
PVB-FNT	–2446.3	–2428.3	–2437.3
AAN-FNT	–2441.4	–2450.6	–2446.0

Theoretical selection of the porogenic solvent

The gas phase predictions are appropriate for many purposes. However, they are inadequate for describing the characteristics of many molecules and systems in solution. Indeed, the properties of molecules can differ considerably between the gas phase and solution. Solvation models based on polarizable continuum dielectrics have proven to be flexible and accurate in particular because the solute is accommodated in a molecular cavity of realistic shape.[29] Thus, the solvent effect was theoretically evaluated using the polarizable continuum model using FNT and MAA as the FM and template molecules, respectively.

The Gibbs energy for the solvent effect was obtained using the same calculation procedure as that previously described for DFT. However, the PCM method considers the Gibbs free energy in solution as the sum of three terms: electrostatic contributions, repulsion-dispersion and cavitation energy.

The magnitudes of ΔG for the interaction of FNT with MAA in different solvents, as well as the solvent dielectric constants, are shown in Table 2. Five solvents were considered: toluene, tetrahydrofuran, dichloromethane, acetonitrile and water. The interaction energies were estimated through ΔG (Gibbs energy difference of the FNT-MAA complex in solvent and in vacuum), and the results are presented in Table 2. The Gibbs binding energy of the complex FNT-MAA calculated in vacuum increases in the presence of solvent, indicating that the solvent acts as a competitor. An ideal solvent should not interact with the template molecule or with the functional monomer. It was verified that water interacts most strongly with the FNT-MAA complex, followed by ACN, DCM, THF and toluene. Therefore, toluene would interfere less in the formation of the FNT-MAA complex.

Table 2. Dieletric constants (ε) and calculated solvent effects (γ) of 1:1 MAA-FNT complexes

Environment	ε	ΔG / (kJ mol^{-1})	γ / (kJ mol^{-1})
Vacuum		–2464.8	–
Toluene	2.4	–2447.3	17.5
Tetrahydrofuran	7.6	–2444.4	20.4
Dichloromethane	8.9	–2433.6	31.2
Acetonitrile	36.5	–2421.5	43.3
Water	78.4	–2410.7	54.1

It was verified that protic solvents with high dielectric constants tend to interfere in the complex formation. Therefore, solvents with low dielectric constants are more appropriate to be used as a porogen in the synthesis of a molecular imprinting polymer. According to Dong *et al.*,[6] molecular modeling of the interaction FM-template considering the solvent effect can help in choosing an appropriate solvent as a complementary approach to the selection experiment.

Polymer characterization

Fourier transform infrared spectroscopy (FT-IR)

FT-IR spectra of (A) PVB-MIP/MAA-MIP and (B) PVB-NIP/MAA-NIP are shown in Figure 2. Both spectra present the same characteristic absorption bands, which indicate that the adopted washing procedure was efficient for removing residual FNT from the polymer and that the imprinted polymer did not incorporate the template molecule into the polymeric structure. Moreover, the NO_2 group of FNT shows intense absorption between 1553 and 1347 cm^{-1} that is related to axial deformation of the asymmetric and symmetric NO_2 group on the aromatic ring of the FNT, which was not observed in the spectra. The main absorption bands are the following: 3444 cm^{-1} (OH stretch for the monomer in the COOH group), 3001 cm^{-1} (OH stretch for the COOH dimer), 1733 cm^{-1} (OH stretch for the ester and COOH), 1639 cm^{-1} (C=C stretch for unreacted vinyl groups), 1400 cm^{-1} (angular deformation of –O–CH_2), and 1267 cm^{-1} (angular deformation of C-O of the ester group). The presence of OH group stretching bands indicates the presence of carboxylic groups in the polymer, which provide the polymer with the ability to form H-bonds with the template.[7]

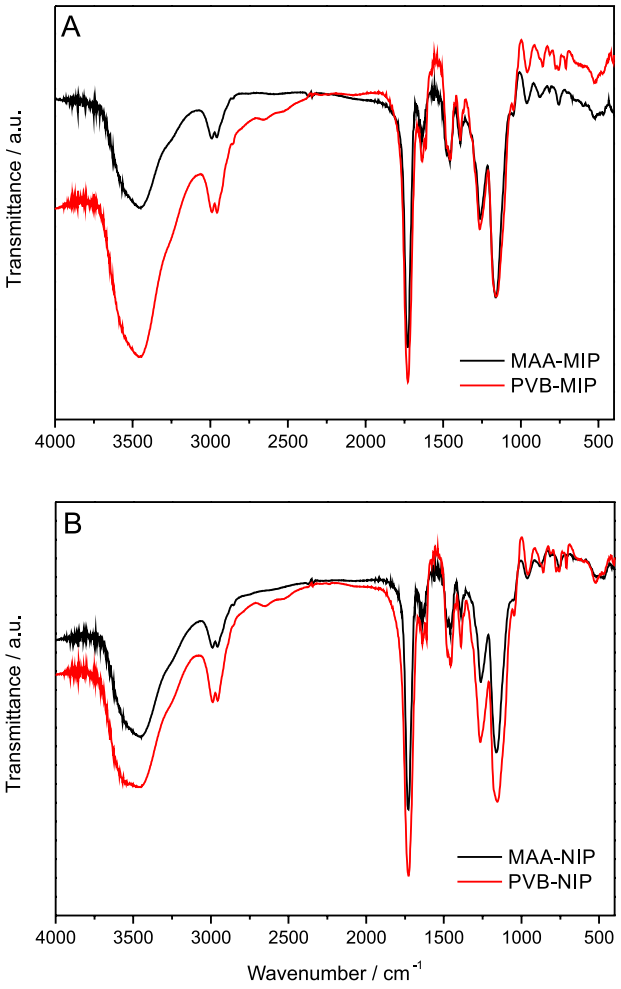

Figure 2. FT-IR spectra of (A) MAA-MIP/PVB-MIP and (B) MAA-NIP/PVB-NIP.

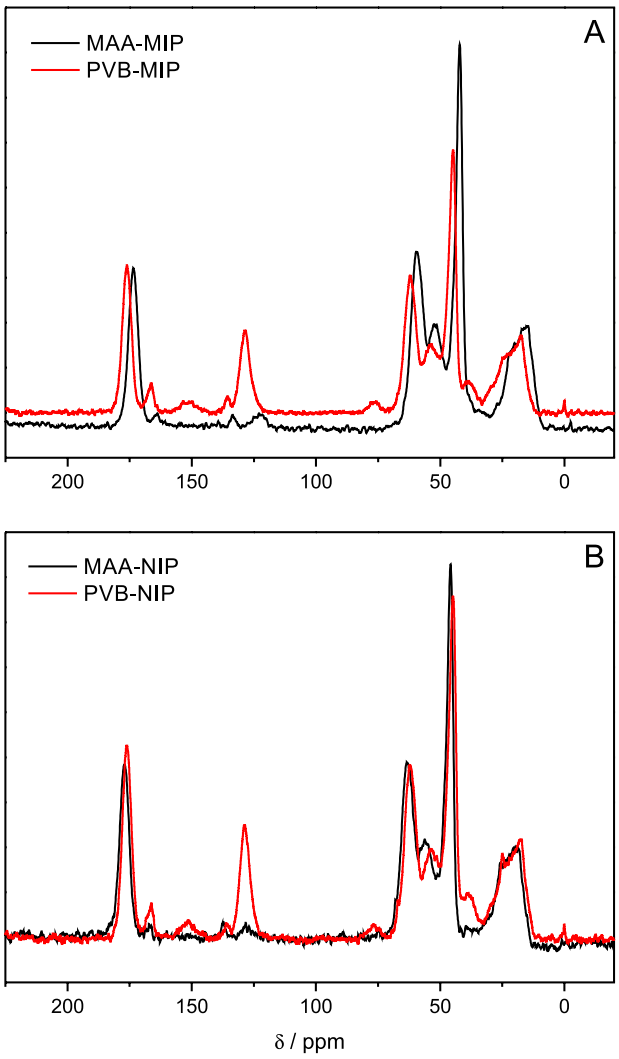

Figure 3. ^{13}C CP-MAS NMR spectra of (A) MAA-MIP/PVB-MIP and (B) MAA-NIP/PVB-NIP.

Cross polarization magic angle spinning nuclear magnetic resonance (CP-MAS NMR)

The ^{13}C CP-MAS NMR spectra (Figure 3) also confirm that both polymeric solids (MIP and NIP) present the same carbonic structure. The main resonances shown are attributed to the following: 20-80 ppm (methyl and methylene groups of EGDMA and FM), 100-130 ppm (unreacted double bonds of the EGDMA) and 160-180 (C=O of EGDMA and FM).[23]

Scanning electron microscopy

Micrographs of the MIP and the corresponding NIP-polymers of the same FM (Figure 4) revealed the existence of appreciable differences in their morphologies. To compare the morphological differences between these polymers, only those synthesized using MAA as a functional monomer will be considered because the polymer obtained with PVB generated polymers with highly irregular morphologies. The micrographs obtained for the polymers synthesized with MAA (Figure 4A-B)

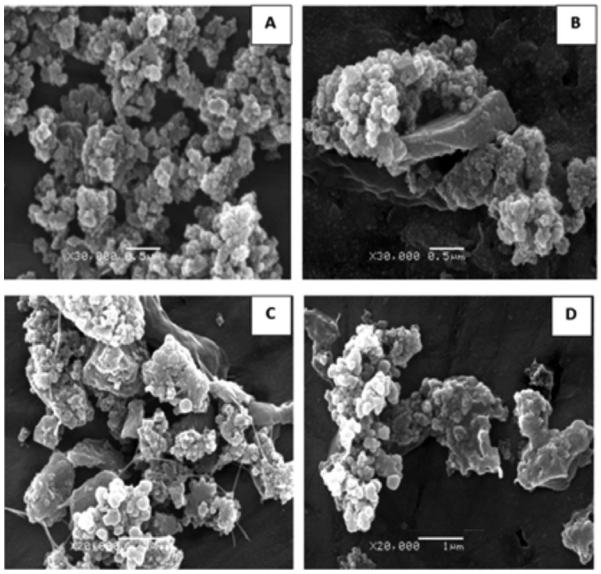

Figure 4. Scanning electron micrographs of (A) MAA-MIP, (B) MAA-NIP, (C) PVB-MIP and (D) PVB-NIP.

showed that the surface of the MIP is very similar to the NIP. The morphology of these polymers is in agreement with several studies using the bulk method to the preparation of these materials.

BET analysis

The porosities of the polymers synthesized with MAA and PVB in toluene were obtained through nitrogen sorption porosimetry. Whereas surface areas were obtained by the BET method, volumes and average pore sizes were calculated by the BJH method. The results are shown in Table 3. The results corroborate with those reported by Farrington and Regan,[11] where the imprinted polymers present a larger surface area than the non-imprinted polymers. Nevertheless, the pore volumes and average pore diameters did not vary to a great extent between the imprinted and non-imprinted polymers; this finding could be attributed to the fact that the polymers were synthesized with the same volume and with the same porogen solvent.

Table 3. Surface areas, pore volumes and pore diameters for MIP and NIP synthesized with MAA or PVB as functional monomers and toluene as porogen solvent

Polymer	Surface area / (m^2 g^{-1})	Pore volume / (cm^3 g^{-1})	Average pore diameter / nm
MAA-MIP	308.0	0.4	5.4
MAA-NIP	267.5	0.3	4.6
PVB-MIP	96.7	0.1	4.5
PVB-NIP	86.6	0.1	4.4

According to the experimentally obtained data, all polymers may be considered as mesoporous because they presented surface areas ranging from 10 to 500 m^2 g^{-1} and pores with average diameters ranging from 2 to 50 nm.

Evaluation of the adsorption efficiency of polymers synthesized with the functional monomers MAA and PVB in toluene

To validate the results obtained by theoretical molecular modeling of FM-FNT interaction, batch rebinding studies were conducted for the best functional monomer (MAA) and the worst functional monomer (PVB), determined from the molecular modeling calculations.

Figure 5 shows the adsorbed FNT on the imprinted and non-imprinted polymers synthesized with MAA or PVB as well as the relative selectivity coefficients (ratio of the adsorbed FNT amount by MIP and NIP).

A large selectivity coefficient (β) indicates good selectivity of the imprinted polymer. The value of β for

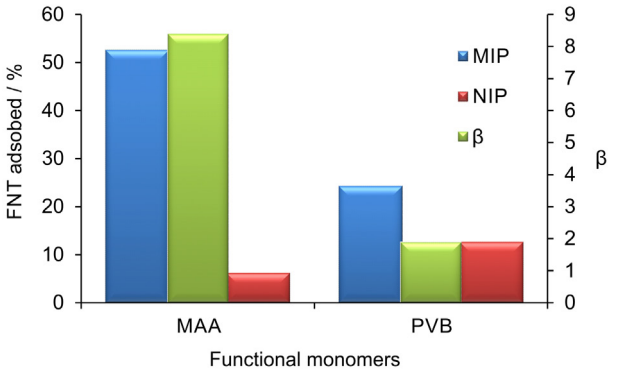

Figure 5. FNT adsorbed by the synthesized MIP and NIP using MAA or PVB as functional monomers and their relative selectivity coefficients (β).

the polymer synthesized with MAA is approximately 8.4, whereas for the polymer synthesized with PVB, the value of β is approximately 1.9. Thus, the theoretical results are verified experimentally, and we can conclude that an imprinted polymer produced using MAA as functional monomer has a higher specificity for selective sites in the molecular recognition process.

Evaluation of the adsorption efficiency of polymers synthesized in different solvents

To validate the theoretical results obtained by molecular modeling studies, polymers synthesized using toluene, DCM and ACN as porogenic solvents were evaluated through batch rebinding studies. For this purpose, the percentages of FNT adsorbed by each polymer synthesized in a different solvent were determined (Figure 6).

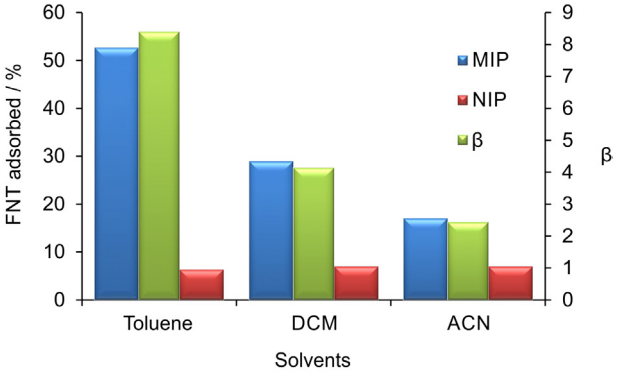

Figure 6. FNT adsorbed by the synthesized MIP and NIP using MAA as functional monomers in different solvents and their relative selectivity coefficients.

The results obtained are in agreement with those obtained using molecular modeling, where toluene was demonstrated to be the most appropriate solvent for the synthesis of the molecularly imprinted polymer FNT-MAA. The MIP synthesized in toluene presents an FNT adsorption of approximately 50% and a relative selectivity coefficient

(β) of 8.4, whereas the MIPs synthesized in DCM and ACN presented a β value of 4.1 and 2.4, respectively. These results corroborate those reported by Kyzas *et al.*,[30] where MIP in hydrophobic organic solvents, such as chloroform or toluene, generally presents a better performance. This finding can be explained by non-polar solvents eliminating non-specific hydrophobic interactions and creating a better environment for electrostatic interactions, which play an important role in molecular recognition. Therefore, toluene, with a lower dielectric constant, will be more adequate for selective FNT recognition by the MIP.

Adsorption isotherms

To characterize the adsorption behavior and the binding site distribution of the MIP synthesized in toluene, using the best and the worst FM (MAA and PVB), the adsorption isotherms of MIPs and NIPs were constructed. For this purpose, the adsorption of FNT by the polymers in ten different concentrations, ranging from 0.5 to 7.5 mmol L^{-1}, was evaluated. The procedure employed was that described previously.

Generally, the adsorption isotherms had been classified into two types, homogeneous (Langmuir) and heterogeneous (Freundlich, Bi-Langmuir and Langmuir-Freundlich), where the heterogeneous models had been widely used to characterize the molecularly imprinted polymer.[5,31]

As observed in Figure 7, the experimental isotherms of the MIP were fitted by Langmuir-Freundlich (LF) because this model can fit both the sub-saturation and saturation regions of the isotherms.[32,33]

This LF model describes the relationship between the equilibrium concentrations of adsorbed per gram (B) and free (F) guest molecules in heterogeneous systems with three different coefficients obtained by the following equation:

$$B = \frac{N_t K F^m}{1 + A F^m} \quad (9)$$

where N_t is the total number of binding sites, A is the average binding and m is the heterogeneous index.

The results presented in Table 4 show that both polymers (MIP) presented a heterogeneity index lower than 1, indicating that the material is heterogeneous and corroborating the results obtained by scanning electron microscopy. The number of binding sites determined for both MIP (MAA-MIP and PVB-MIP) was higher than those measured for the respective NIPs, indicating that the MIPs have a greater number of binding sites available. In addition, it was verified that the MIP synthesized with MAA presented twice the number of binding sites as the MIP synthesized with PVB.

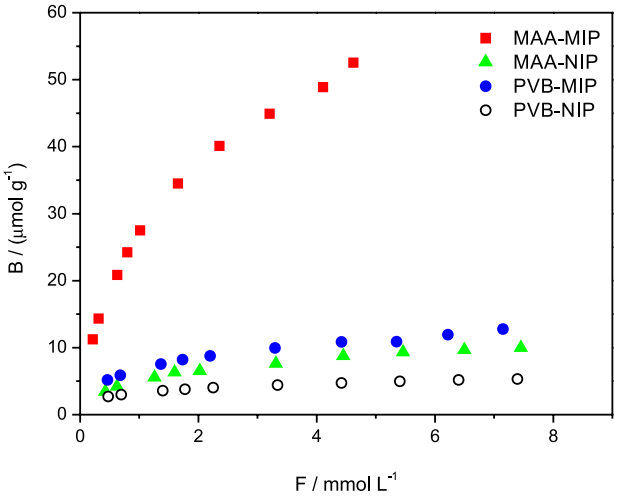

Figure 7. Adsorption isotherms of MIP and NIP (MAA and PVB functional monomers) using the Langmuir-Freundlich model. B is the concentration of FNT retained/polymer concentration × 1000; F is the concentration of the free FNT.

Table 4. Coefficients of the Langmuir-Freundlich isotherms for MIP synthesized with MAA or PVB as functional monomers and toluene as porogen solvent

Polymer	N_t / (µmol g^{-1})	A / (mmol^{-1} L)	m	r
MAA-MIP	103.35	0.354	0.680	0.999
PVB-MIP	53.773	0.144	0.375	0.990

N_t: total number of binding sites; A: average of binding affinity; m: heterogeneity index; r: correlation coefficient.

Selectivity of MIP by solid phase extraction

The selectivity of the FNT-imprinted polymer was evaluated following a previously optimized MISPE procedure.[28] The recovery of FNT and its analogues after fortifying blank tomato samples, using MIP and NIP were evaluated. The recovery values obtained after the washing and elution steps by the imprinted and non-imprinted polymers are shown in Table 5.

Table 5. Recovery of FNT and its analogs by MIP and NIP

	Recovery / %			
	MIP		NIP	
	Washing	Elution	Washing	Elution
FNT	N/D	98	94	3
PT	90	N/D	88	N/D
MPT	92	N/D	91	3
FT	89	4	90	N/D

N/D: not detected.

It was verified that the analogous FNT were mainly removed from the MISPE cartridge at the washing step and FNT was recovered at the elution step, using the optimized experimental conditions described previously. These results confirm the selectivity of the synthesized MIP to FNT even when this compound is present in a complex food matrix in the presence of other FNT-analogous substances. In addition, FNT showed non-affinity for the synthesized NIP.

Conclusions

Molecular modeling based on DFT proved to be a powerful tool to select the functional monomer for the synthesis of a molecularly imprinted polymer for FNT recognition. The experimental results showed that the MIP synthesized with the predicted best FM (MAA) presented a selectivity coefficient approximately 4 times higher than that synthesized with PVB, which was predicted to be the worst FM. Toluene was shown to be the best solvent for the stabilization of the pre-polymerization complex. The solvent effect was evaluated by analysis of the solvent interference in the complex formation between the FNT and MAA in the synthesis of MIP. Batch rebinding experiments were performed by the synthesis of different imprinted polymers, using MAA and PVB as functional monomers and toluene, dichloromethane and acetonitrile as porogens to validate these approaches.

The experimental results obtained confirmed the data predicted by molecular modeling.

Methacrylic acid and toluene were determined to be the combination of functional monomer and solvent, respectively, that leads to the most stable complex for FNT-imprinting.

The MIP synthesized showed suitable properties for use in molecularly imprinted solid phase extraction and was successfully applied for the selective determination of FNT in tomatoes.

Acknowledgements

The authors gratefully acknowledge financial support from CNPq (141618/2010-8) and FAPESP (2007/02306-9).

References

1. Dineiro, Y.; Menendez, M. I.; Blanco-Lopez, M. C.; Lobo-Castanon, M. J.; Miranda-Ordieres, A. J.; Tunon-Blanco, P.; *Biosens. Bioelectron.* **2006**, *22*, 364.
2. Liu, Y.; Wang, F.; Tan, T. W.; Lei, M.; *Anal. Chim. Acta* **2007**, *581*, 137.
3. Cormack, P. A. G.; Elorza, A. Z.; *J. Chromatogr. B* **2004**, *804*, 173.
4. Qiao, F. X.; Sun, H. W.; Yan, H. Y.; Row, K. H.; *Chromatographia* **2006**, *64*, 625.
5. Yan, M.; Ramström, O.; *Molecularly Imprinted Materials: Science and Technology*; Marcel Dekker: New York, 2005.
6. Dong, W. G.; Yan, M.; Liu, Z.; Wu, G. S.; Li, Y. M.; *Sep. Purif. Technol.* **2007**, *53*, 183
7. Dong, W. G.; Yan, M.; Zhang, M. L.; Liu, Z.; Li, Y. M.; *Anal. Chim. Acta* **2005**, *542*, 186.
8. Dineiro, Y.; Menendez, M. I.; Blanco-Lopez, M. C. ; Lobo-Castanon, M. J.; Miranda-Ordieres, A. J.; Tunon-Blanco, P.; *Anal. Chem.* **2005**, *77*, 6741.
9. Yao, J. H.; Li, X.; Qin, W.; *Anal. Chim. Acta* **2008**, *610*, 282.
10. Wu, L. Q.; Sun, B. W.; Li, Y. Z.; Chang, W. B.; *Analyst* **2003**, *128*, 944.
11. Farrington, K.; Regan, F.; *Biosens. Bioelectron.* **2007**, *22*, 1138.
12. Okutucu, B.; Telefoncu, A.; *Talanta* **2008**, *76*, 1153.
13. Wu, L. Q.; Zhu, K. C.; Zhao, W. P.; Li, Y. Z.; *Anal. Chim. Acta* **2005**, *549*, 39.
14. Kowalska, A.; Stobiecka, A.; Wysocki, S.; *J. Mol. Struc.-Theochem* **2009**, *901*, 88.
15. Saloni, J.; Lipkowski, P.; Dasary, S. S. R.; Anjaneyulu, Y.; Yu, H.; Hill Jr., G.; *Polymer* **2011**, *52*, 1206.
16. Chianella, I.; Karim, K.; Piletska, E. V.; Preston, C.; Piletsky, S. A.; *Anal. Chim. Acta* **2006**, *559*, 73.
17. Raghavachari, K.; Anderson, J. B.; *J. Phys. Chem* **1996**, *100*, 12960.
18. Chen, L. N.; Jia, X. J.; Lu, Q.; Peng, Y.; Du, S. H.; Chen, Q.; *Sep. Purif. Technol.* **2010**, *71*, 324.
19. Nicholls, I. A.; *Chem. Lett.* **1995**, *24*,1035.
20. Nicholls, I. A.; *J. Mol. Recognit.* **1998**, *11*, 79.
21. Searle, M. S.; Williams, D. H.; Gerhard, U.; *J. Am. Chem. Soc.* **1992**, *114*, 10697.
22. Williams, D. H.; Cox, J. P. L.; Doig, A. J.; Gardner, M.; Gerhard, U.; Kaye, P. T.; Lal, A. R.; Nicholls, I. A.; Salter, C. J.; Mitchell, R. C.; *J. Am. Chem. Soc.* **1991**, *113*, 7020.
23. Spivak, D. A.; *Adv. Drug Deliver. Rev.* **2005**, *57*, 1779.
24. Gholivand, M. B.; Khodadadian, M.; Ahmadi, F.; *Anal. Chim. Acta* **2010**, *658*, 225.
25. Khodadadian, M.; Ahmadi, F.; *Talanta* **2010**, *81*, 1446.
26. Frisch, M. J.; Trucks, G. W.; Schlegel, H. B.; Scuseria, G. E.; Robb, M. A.; Cheeseman, J. R.; Zakrzewski, V. G.; Montgomery, J. J. A.; Stratmann, R. E.; Burant, J. C.; Dapprich, S.; Millam, J. M.; Daniels, A. D.; Kudin, K. N.; Strain, M. C.; Farkas, O.; Tomasi, J.; Barone, V.; Cossi, M.; Cammi, R.; Mennucci, B.; Pomelli, C.; Adamo, C.; Clifford, S.; Ochterski, J.; Petersson, G. A.; Ayala, P. Y.; Cui, Q.; Morokuma, K.; Malick, D. K.; Rabuck, A. D.; Raghavachari, K.; Foresman, J. B.; Cioslowski, J.; Ortiz, J. V.; Stefanov, B. B.; Liu, G.; Liashenko, A.; Piskorz, P.; Komaromi, I.; Gomperts, R.; Martin, R. L.; Fox, D. J.; Keith, T.;

Al-Laham, M. A.; Peng, C. Y.; Nanayakkara, A.; Gonzalez, C.; Challacombe, M.; Gill, P. M. W.; Johnson, B.; Chen, W.; Wong, M. W.; Andres, J. L.; Gonzalez, C.; Head-Gordon, M.; Replogle, E. S.; Pople, J. A.; *GAUSSIAN 03*, Revision C.01; Gaussian Inc, Pittsburgh, PA, 2003.

27. Pereira, L.; Rath, S.; *Anal. Bioanal. Chem.* **2009**, *393*, 1063.
28. de Barros, L. A.; Martins, I.; Rath, S.; *Anal. Bioanal. Chem.* **2010**, *397*, 1355.
29. Foresman, J. B.; Frisch, A.; *Exploring Chemistry with Electronic Structure Methods*, 2nd ed.; Gaussian Inc.: Pittsburg, PA, 1996.
30. Kyzas, G. Z.; Bikiaris, D. N.; Lazaridis, N. K.; *Chem. Eng. J.* **2009**, *149*, 263.
31. Umpleby, R. J.; Baxter, S. C.; Rampey, A. M.; Rushton, G. T.; Chen, Y. Z.; Shimizu, K. D.; *J. Chromatogr. B* **2004**, *804*, 141.
32. Tamayo, F. G.; Casillas, J. L.; Martin-Esteban, A.; *Anal. Chim. Acta* **2003**, *482*, 165.
33. Rushton, G. T.; Karns, C. L.; Shimizu, K. D.; *Anal. Chim. Acta* **2005**, *528*, 107.

Submitted: August 28, 2013
Published online: January 17, 2014

FAPESP has sponsored the publication of this article.